ON THE TURBULENCE OF A REATTACHING SEPARATED FLOW WITH THE EXISTENCE OF GAS INJECTION

Harinaldi, T. Ueda, A. Matsuo and M. Mizomoto
Department of Mechanical Engineering
Graduate School of Science and Technology, Keio University
3-14-1 Hiyoshi, Kohoku-ku, Yokohama 223-8522, Japan

ABSTRACT

An experimental study on a reattaching separated flow over a backward facing step with a nitrogen gas injection from a slit port to the recirculating zone has been conducted by means of flow measurement and visualization. The mean velocity, the turbulent intensity obtained from the fluctuating velocity in streamwise and cross-stream direction and the Reynolds shear stress have been measured using a laser Doppler velocimeter. A laser-sheet based visualization has been made to demonstrate the complex nature of the flow field. In the experiments, the free stream velocity was kept constant at 10 m/s and the specific momentum ratio between the injected gas and main airflow was varied by changing the injection velocity. Two cases of injection location have been investigated, one at a near step and another one at a near reattachment location. The profiles of measured turbulent properties show that as the specific momentum ratio of the injection is increased, the turbulent intensity and the Reynolds shear stress increase in the shear layer region, while they tend to decrease in the reverse flow zone. These effects are more pronounced in case of the gas is injected at the near step location. Further assessment on recorded images suggest that changing the specific momentum of injection alters the injected jet behavior with respect with its fluctuation, mixing with the airflow as well as the dimensionality of its growth.

INTRODUCTION

Reattaching separated flow over a sudden expansion of a backward facing step constitutes a fundamental test case for research works in a wide range of field such as fluid mechanics, heat transfer, combustion and so on. It has been a long time history of research on various key features of the flow structure, either in the form of theoretical and experimental works (Etheridge and Kemp, 1978; Eaton and Johnston, 1981; Reulet et al., 1995), or in computational studies, which recently becomes a growing interest (Abe et al, 1994; Kobayashi and Togashi, 1996). However, most of them were dealing with the case of no mass addition to the flow field. Relatively limited studies have been done to the case where mass injection is issued to the flow field. Among them, intensive studies on a back-step flow with mass addition from porous plate had been done by Yang's group which included experimental measurements on velocity field (Yang et al., 1994), and high-temperature heat transfer (Yang and Tsai, 1996). A numerical study on the similar flow condition was made by Yang and Kuo (1997). Haibel and Mayinger (1994) had investigated the effect of injection angle and injector geometry to the cold and reactive mixing of gas injected upstream of a step by holographic interferometer visualization.

Whereas in fact, for a combustor application, one of major importance is the mixing process between the injected fuel and the surrounding air that is controlled by convective mass transfer and diffusion mechanism. These all are very much influenced by several factors such as the structure of turbulence in the flow field, the dynamic nature of the injected gas and also the geometry of injector, which has not yet been thoroughly elucidated. Thus, the present study has the following purposes:

- to investigate the flow characteristics and turbulence structure in the separated shear layer and recirculation region under the existence of gas injection to the flow field,
- to get a better understanding of the fundamental mechanism and turbulence influence on gas-air mixing process focussing on the development, mixing, and fluctuation behavior of the injected gas and
- to obtain new experimental data and information that may be used to develop computational models.

2. EXPERIMENTAL METHOD

2.1 Experimental Apparatus

A sketch of the present experimental apparatus and instrumentation appears in Fig. 1. The experiments were conducted in a small-scale low turbulence wind tunnel configuration ($(u^2)^{1/2}/U \cong 0.7$ percent in the free stream), with injection gas flow system and particle seeding supply system. The dimensions of test section were 50 x 80-mm^2 cross section upstream of a 20 mm-height step and 300 mm long down stream of the step. A slit injection port with 1-mm width spanned across the test section at a distance l_f from the step was installed at the base wall of the test section. The coordinate system was set as shown in the figure.

Scattering particles were droplets of Dymethil Silicon oil in the order 1~2 μm. In velocity measurement, particle was seeded directly to airflow system, meanwhile for visualization it was seeded to the injected gas supply system.

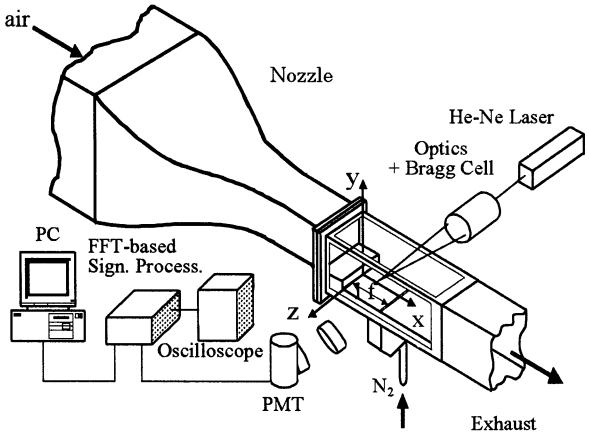

Figure 1. Experimental Set up

2.2 Instrumentation

2.2.1 Velocity Measurement. A dual beam, forward-scattering laser Doppler velocimeter (LDV) with a Bragg cell to detect flow reversal was used to measure a mean velocity and a turbulent intensity of velocity fluctuation. A 15-mW He-Ne laser was used as light source. Doppler signals were detected by a photomultiplier and processed with a FFT spectrum analysis-based digital signal processor (Kanomax DSP 8007) interfaced with a personal computer. The mean velocity (U and V) and turbulent intensity of a fluctuating velocity (u' and v') were calculated from direct measured data. The cross-stream velocity component was measured by rotating the LDV optics 90 deg. Whilst, the correlation ($\overline{uv}$) was calculated by

$$\overline{uv} = 1/2\left(u'^2_+ - u'^2_-\right) \qquad (1)$$

where u'_+ and u'_- are the turbulent intensities of fluctuating velocities in +45 and –45 degree inclined to the streamwise direction, respectively. Infrequent but not negligible spurious data that were included in the stored data in the computer memories were reduced by ε–σ method (ε =6), following Ueda (1982).

By selecting appropriate values of Bragg cell shift frequency, the filter, gain, trigger of the signal processor and so on, and with realization more than 4000 data points for each measurement station, the measurement uncertainties were estimated to be ±3 % for the mean velocity, ±5 % for the turbulent intensity of fluctuating velocity and, ±13 % for Reynolds shear stress.

2.2.2 Flow Visualization. A 0.4 mm-thickness and 100 mm-width laser sheet was made in the plane of visualization by passing the laser beam from a pulsed Nd:Yag Laser (Spectra-Physics GSR: pulse frequency 10 Hz, 200 MJ/pulse at wave length 532 nm) through a cylindrical lens arrangement. A CCD camera (Sony Hi-8-VX1 : shutter speed 1/1000 s, frame rate 30 fps) was used to capture a very clear and instantaneous features of the flow field image that could grabbed even spatially dynamic processes with high resolution. This made possible since the exposure time of the image was solely determined by the laser emission time width (6-7 ns). The recorded images were transmitted to a personal computer for further analysis.

2.3 Experimental Conditions

In the present study, the free air stream velocity ahead of the step was maintained at U_o= 10 m/s, corresponds to a Reynolds number based on the step height (U_o.H/ν_{air}) about 1.25 x 10^4. The parameters were the specific momentum ratio between the injected gas and main airflow ($I = \rho_{N2}V_{N2}^2 / \rho_{air}U_o^2$) and the injection distance from the step (l_f). Two different injection position at l_f = 40 mm (l_f /H = 2) and l_f = 80 mm (l_f/H = 4) were selected, and for each position the specific momentum ratio of injection was varied (I = 0.01, 0.04, 0.1 and 0.3) by altering nitrogen injection velocity at constant main airflow velocity (V_{N2} = 1, 2, 3.2 and 5.6 m/s). The LDV measurements were conducted at x/H = 1 ~ 3 in case injection at l_f /H = 2, and at x/H = 3 ~ 5 in case injection at l_f /H = 4. The velocity data were obtained in the range y/H = 0.1 ~ 2. Meanwhile, the visualizations of the flow field were conducted at vertical center plane (z/H = 0), and several horizontal planes (y/H = 0.1 ~ 1).

3. RESULTS AND DISCUSSION

3.1 Initial Condition

Velocity measurement of initial upstream condition was done at position x = - 2 mm from the step. Velocity profile shows a uniform flow with turbulent intensity about 0.7 percent. The boundary layer has a rather high turbulence level, with maximum turbulent intensity about 3 percent. The thickness of the boundary layer before the separation is about 3 mm (δ/H = 0.15). Determination of reattachment length without injection obtained a location with zero mean horizontal velocity at 0.05H above the wall which is defined as reattachment point (x_r) at 5.5 H from the step.

3.2 Mean Velocity Profiles

Effects of various ratios of specific momentum injections to the mean streamwise velocity profiles are compared

between two cases of injection location in Figs. 2(a) and 2(b). When the nitrogen gas is issued at $l_f/H = 2$, Fig. 2(a) shows that as the injection momentum is increased, near the base wall area ($y/H < 0.15$), except at $x/H = 1$, the reverse flow velocity slightly decreases. This trend is similar to that of porous mass addition investigated by Yang et al. (1994). The horizontal momentum conservation makes the creation of mass increase due to gas addition is balanced by a decrease in velocity. However, apart from the base wall area the behavior differs from porous injection case. In the present profiles, as specific momentum injection is increased, within recirculating zone the velocity of positive flow part decreases whilst the velocity of reverse flow part increases so that the locations of the dividing streamline shift up and the recirculation zone size increases. This suggests that the vertical penetration of momentum of the injected gas being more significant in the recirculation zone. The momentum penetration is supposed to be coupled by an increase of static pressure in the recirculating zone which make a decrease in pressure difference across the shear layer. As a result the size of the recirculation zone increases.

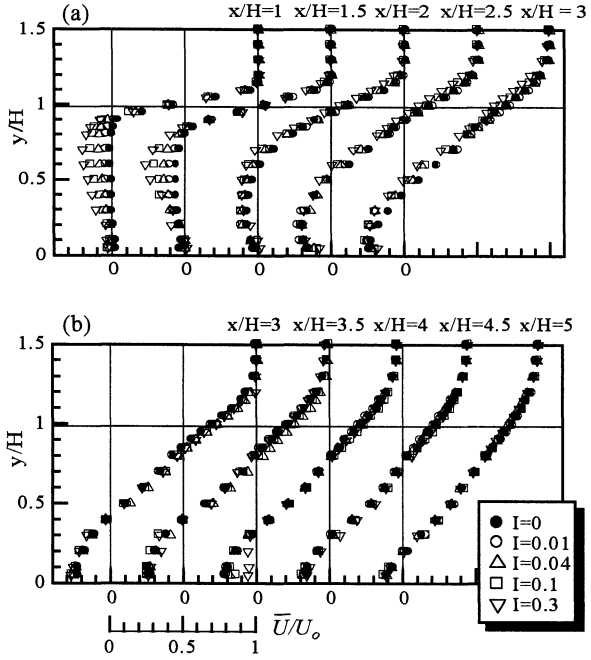

Figure 2. Mean Streamwise Velocity Profiles with Nitrogen Injection at (a) $l_f/H = 2$, (b) $l_f/H = 4$. (U_o= 10 m/s ; z/H = 0)

On the other hand, in case of injection is done at a location near reattachment region ($l_f/H = 4$), Fig. 2(b) shows that all the profiles are almost coincident at all locations except at the near wall of injection point where the reverse flow velocity reduces. This indicates that as the reverse flow velocity is higher and turbulence is stronger in the reattachment region, the injected gas flow become less momentous than the flow in recirculation zone.

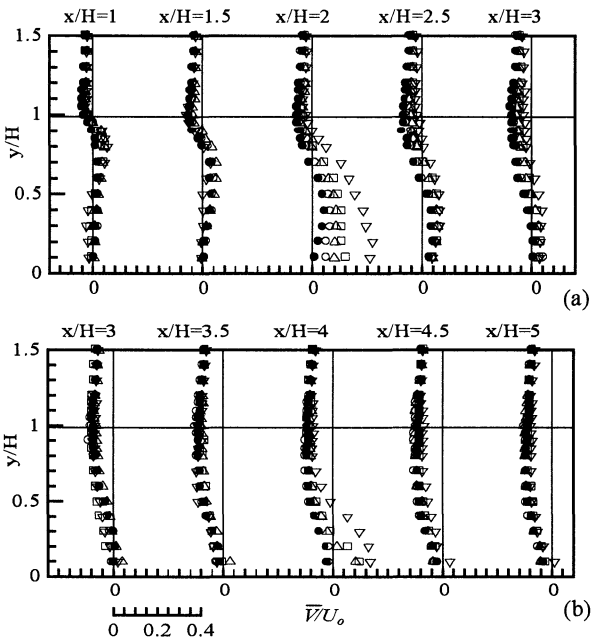

Figure 3. Mean Cross-stream Velocity Profiles with Nitrogen Injection at (a) $l_f/H = 2$, (b) $l_f/H = 4$. (U_o= 10 m/s ; z/H = 0 ; Legends refer to Figure 2).

Meanwhile the mean cross-stream velocity profiles shown in Figs. 3(a) and 3 (b) indicate that in case the near-step injection, as the momentum injection is increased the vertical velocity also increases and the position where it changes sign from positive ($V > 0$) to negative ($V < 0$) shifts upward. However, this tendency is not remarkably observed for the near-reattachment point injection except for the profiles at stream wise location of injection point ($x/H = 4$). These results are expected when one considers which dominant flow governing the flow field by taking into account the specific momentum of injection as well as the location of injection point.

3.3 Turbulence Properties

3.3.1 Turbulent Intensities. The profiles of turbulent intensity that is determined from the stream wise and cross-stream component of the fluctuating velocities (u and v) are depicted in Figs. 4(a) and 4(b). The turbulent intensity is expressed as follows:

$$TI = \sqrt{\frac{\overline{u^2} + \overline{v^2}}{2}} \qquad (2)$$

and it is normalized by the main air flow velocity (U_o).

The effects of increasing the specific momentum ratio of the injection are more remarkable in case of near step injection compared to the case of near reattachment point injection. Relatively more significant change of the turbulence level is observed compared to the change of mean velocity for every case of injection. The profiles show two regions with different trends of turbulent intensity change

due to an increase of injection momentum. Near the base wall the turbulent intensity is suppressed by increasing the injection momentum. All curves of the profiles then converge upward to a certain point located in the lower side of the shear layer. In case injection at $l_f/H = 2$, this point slightly decreases from y/H = 0.7 at x/H = 1 to y/H = 0.55 at x/H = 3, and for injection at $l_f/H = 4$ the point varies from y/H = 0.5 at x/H = 3 to y/H = 0.1 at x/H = 4.5. Thus, the decrease of the points follows the growth of the shear layer along stream wise direction. Only up to this region, the trend is qualitatively similar to that found by Yang et al. (1994).

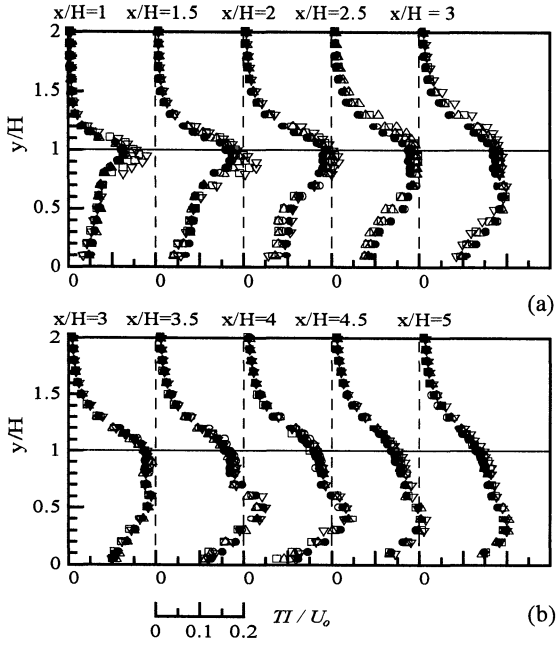

Figure 4. Profiles of Turbulent Intensity of Fluctuating Velocity with Nitrogen Injection at (a) $l_f/H = 2$, (b) $l_f/H = 4$. (U_o= 10 m/s ; z/H = 0 ; Legends refer to Figure 2).

On the other hand, above this point, the curves diverge indicating that in the shear layer region, the turbulence is stronger as the injection momentum is increased. The results qualitatively agree to the numerical prediction made by Yang and Kuo (1997) despite the different injection condition. The augmentation of the turbulent intensity even takes place until the boundary region between the shear layer and the free stream, which suggest a deep penetration of the injected gas. Furthermore, the increase of turbulent intensity in the shear layer is lower in case of near reattachment injection.

3.3.2 Reynolds Shear Stress Profiles. In their review, Eaton and Johnston (1981) had summarized data of the maximum Reynolds shear from various measurements in no mass addition case that are rather scattered, and they figured out that the acceptable data lies between a certain envelope of value. Outside the envelope they suggested that the data encountered some problem in the measurement. Figs. 5(a) and 5(b) show some important characteristics of Reynolds shear stress distributions of our present measurement. In the figures the vertical dash lines show the envelope of acceptable maximum value of Reynolds shear stress (Eaton and Johnston, 1981). All the data in case of no injection occurs fall inside the envelope, which suggest the reliability of our present measurement. Thus, the deviation of the Reynolds shear stress beyond the envelope is considered as the effects of the gas injection.

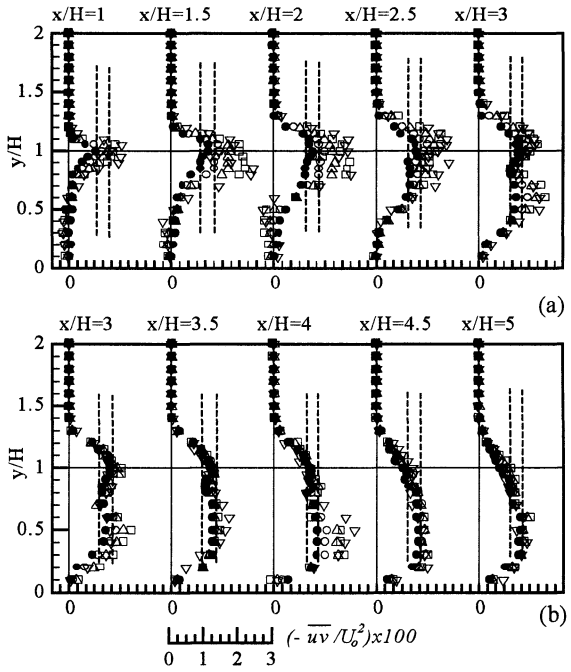

Figure 5. Profiles of Reynolds Shear Stress with Nitrogen Injection at (a) $l_f/H = 2$, (b) $l_f/H = 4$. (U_o= 10 m/s ; z/H = 0 ; Legends refer to Figure 2).

Fig. 5(a) shows that within the shear layer region the Reynolds shear stress is maintained at high level value as the velocity gradient and velocity fluctuation are also high. By increasing the injection momentum the Reynolds shear stress becomes higher and the maximum value goes beyond the envelope. The change of the Reynolds shear stress is relatively more intense compared to the change of the turbulent intensity. On the other hand, in the lower side of the recirculation zone i.e. the region near the wall, only a slight change of Reynolds shear stress can be observed at the location of injection and its upstream (x/H = 1 ~ 2), with a tendency that the value decreases. Negative values of Reynolds shear stress are observed for injection with high specific momentum ratio for example at y/H less than 0.5 for I = 0.1 and 0.3. These negative values are consistent with the mean profiles of stream wise velocity, which have negative gradient ($\partial\overline{U} / \partial y < 0$) in the region. Moreover, the Reynolds shear stress profiles are also expected to exhibit negative value at the location very near the base wall (y/H < 0.1). However, since the LDV optics were rotated 45 degree, one

of the laser beams was blocked by the base wall, and the data could not be collected in this region.

Meanwhile, Fig. 5(b) shows a qualitatively similar behavior of the Reynolds shear stress variation due to the increase of injection momentum, except that no negative value of Reynolds shear stress can be observed for all condition. Although quantitatively the degree of change is less than the near step injection case, in the shear layer the Reynolds shear stress also increases as injection momentum is increased. A decrease in Reynolds shear stress also takes place in the region near the wall, however it is limited to the location upstream and near to the injection point (x/H = 3.5 and 4).

3.4 Growth Behavior of Injected Gas

Some typical sets of photographs of flow visualization in case of nitrogen gas is issued at $l_f/H = 2$ are presented in Figs. 6(a-f). The photographs include images taken at center plane and horizontal planes. Figs. 6(a-c) represent a low specific momentum injection (I = 0.04), and Figs. 6(d-f) represent a high specific momentum injection (I = 0.3). The figures display the difference of injected gas behavior with respect to the trajectory development, the effect to the dimensionality of flow field, and spanwise growth pattern of injected gas, due to specific momentum variation of injected gas. At low momentum injection (I = 0.04), a spatially quite wavy trajectory of the injected gas suggests a strong influence of the recirculating flow to the jet growth before it reaches the shear layer region and intensely mixes with the airflow. A remarkable three-dimensional growth of the injected gas can be understood from the observation of trajectory pattern in horizontal plane images. At higher y/H (=0.5), the jet flow grows with a manner showing a swirling motion. Shih and Ho (1994) had reported their finding on the generation of two spanwise vortices in back-step flow in water channel with aspect ratio, AR = 3. Although our flow configuration has larger aspect ratio (AR = 4), it is still relatively small so that we supposed the mechanism of the low momentum jet growth can be attributed to the similar formation of the spanwise counter rotating vortex pair induced in the shear layer. Furthermore, temporal assessment shows that the jet fluctuates intensely with trajectory oscillate toward upstream and down stream direction in a fashion indicating periodic manner. As the specific momentum of gas injection is increased (I = 0.3), the injected gas grows with a more upright trajectory and it penetrates the shear layer more deeply. Unlike low momentum injection case, images taken at horizontal planes indicate that the injected gas grows two-dimensionally. Thus, increasing the specific momentum of slit injection intensify the two-dimensionality of the flow field.

Another striking feature that is revealed by the images is the effects of gas injection to the generation of coherence structure inside the shear layer region. A very clear coherence structure, which is generated by the velocity gradient inside the shear layer can be observed in case of I = 0.04. On the other hand, in case of I = 0.3, the formation of the structure tends to be diminished. A closer looks at the velocity gradient ($\partial\overline{U}/\partial y$) at the region where the value is maximum in the shear layer (y/H = 0.9~1.1), and the shear instability leading to the formation of coherence structure is supposed to starts to occur is presented in Fig. 7. The gradient has been estimated from:

$$\left(\frac{\partial \overline{U}}{\partial y}\right)_i = \frac{1}{2}\left(\frac{\overline{U}_{i+1}-\overline{U}_i}{y_{i+1}-y_i}+\frac{\overline{U}_i-\overline{U}_{i-1}}{y_i-y_{i-1}}\right) \qquad (3)$$

where the subscripts *i-1*, *i*, and *i+1* denote consecutive measurement point. The figure shows a significant decrease of velocity gradient at x/H = 1.5 of the region of interest. At x/H = 2 the decrease is less significant and further down stream no remarkable change is observed. This indicates that as the injection momentum is increased, the injected gas reaches the vicinity of location where the first swirling structure is induced, resulting in the decrease on velocity gradient. This obstructs the generation or the convection of the swirling structure.

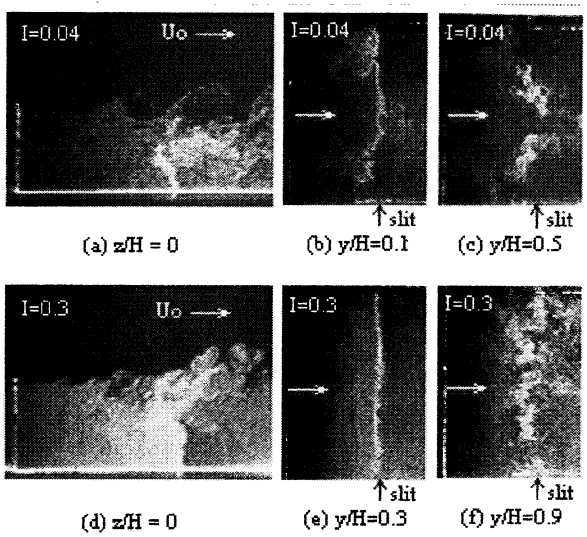

Figure 6. Effects of Specific Momentum Ratio on the Development of the Injected Gas in Case of Injection at $l_f/H=2$

Other sets of pictures for the case of injection near reattachment point ($l_f/H = 4$), are presented in Figs. 8(a-c) for I = 0.04 and Figs. 8(d-f) for I = 0.3. The gas injected with low specific momentum (I = 0.04) deflected strongly toward upstream direction without deep penetration and mix rapidly with the recirculating air flow due to the strong turbulence and high reverse velocity of the flow in the vicinity of injection point. Meanwhile, more extensive growth of the injected gas which penetrates through the shear layer can be observed in case of I = 0.3. Similar trends to near step injection case regarding the effect of specific momentum of injection to the dimensionality of the jet growth can be observed in the images. Furthermore, as the location of

injection point is sufficiently apart from the step, the generation of the coherence structure within the shear layer is not disturbed by the gas injection as their presence are observed in every cases.

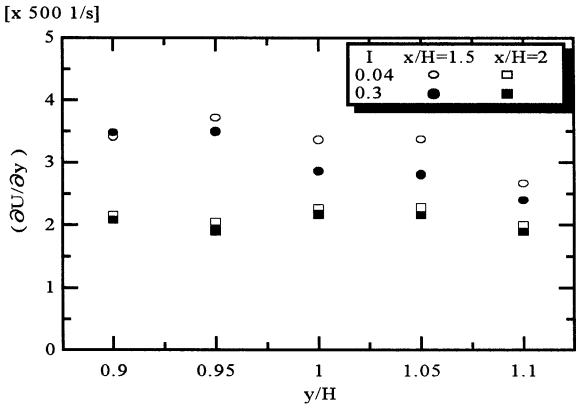

Figure 7. Velocity Gradient in the Vicinity of the Location where the Shear Instability leads to the Formation of Coherence Structure, in case the Injection at l_f/H = 2.

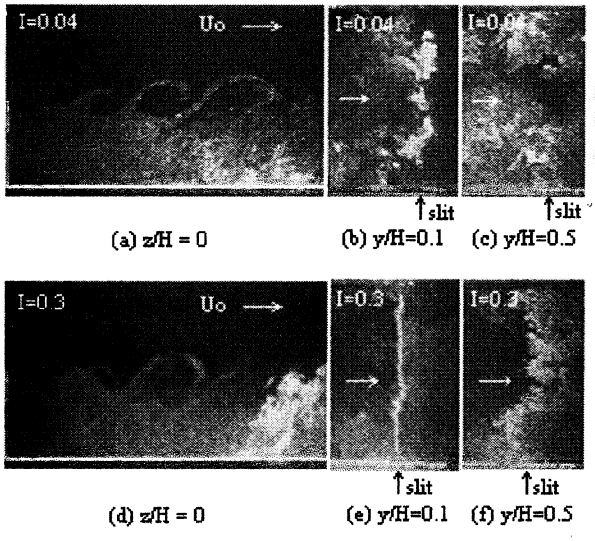

Figure 8. Effects of Specific Momentum Ratio on the Development of the Injected Gas in Case of Injection at l_f/H=4

CONCLUSIONS

A measurement of velocity and a visualization of the flow field behind a backward facing-step with the existence of gas injection have been done to elucidate the turbulence structure and the growth behavior of the injected gas. The results show that as the specific momentum ratio of the injection is increased: (i) the turbulent intensity and the Reynolds shear stress increase in the shear layer region, while they tend to decrease in the reverse flow zone, (ii) the injected gas less fluctuates and penetrates deeper through the flow field, and it tend to restrain the generation of the coherence structure in the shear layer. These effects are more prominent in case of gas is injected at the near step location compared to when injected near to reattachment point, (iii) the two-dimensionality of the flow field as well as the injected gas growth pattern are intensified.

Furthermore, there are some qualitative similar result of turbulence features between the slit gas injection in the present study with those of the porous plate mass addition reported by Yang et al. (1994), especially in the near wall region. However, the trends are different in the shear layer.

REFERENCES

Abe, K., Kondoh, T., and Nagano, Y., 1994, "A New Turbulence Model for Predicting Fluid Flow and Heat Transfer in Separating and Reattaching Flow. 1. Flow-field Calculations," *Int. J. Heat and Mass Transfer*, Vol. 37, pp. 139-151.

Eaton, J.K., and Johnston, J.P., 1981, "A Review of Research on Subsonic Turbulent Flow Reattachment," *AIAA Journal*, Vol. 19, pp. 1093-1099.

Etheridge, D.W., and Kemp, P.H., 1978, "Measurement of Turbulent Flow Downstream of a Rearward-facing Step," *Journal of Fluid Mechanics*, Vol 86, pp. 545-566.

Haibel, M., and Mayinger, F., 1994, "The Effect of Turbulent Structures on the Development of Mixing and Combustion Processes in Sub- and Supersonic H_2 Flames," *Int. J. Heat Mass Transfer*, Vol.37, Suppl. 1, pp. 241-253

Kobayashi, T., and Togashi, S., 1996, "Comparison of Turbulence Models Applied to Backward-facing Step Flow," *JSME Int. J. Ser. B.*, Vol. 29, No. 3, pp. 453-460.

Papadopoulos, G., and Otugen, M.V., 1995, "Separating and Reattaching Flow Structure in a Suddenly Expanding Rectangular Duct," *Trans. ASME, Journal of Fluids Engineering*, Vol. 117, pp. 17-23

Reulet, P., Dumoulin, J., and Millan, P., 1995, "Experimental Investigation of a Flow Behind a Backward-facing Step by Tomographic Visualization, Laser Velocimetry and Infrared Thermography Measurement," *ASME-FED, Experimental and Numerical Flow Visualization*, Vol. 218, pp.171-180

Shih,C., and Ho, C.M, 1994, "Three-dimensional Recirculation Flow in a Backward Facing Step," *Trans. ASME, Journal of Fluids Engineering*, Vol.116, pp.228-232

Ueda, T., Mizomoto, M., Ikai, S., and Kobayashi, T., 1982, "Velocity and Temperature Fluctuations in a Flat Plate Boundary Layer Diffusion Flame," *Combustion Science and Technology*, Vol. 27, pp. 133-142.

Yang, Y.T, and Kuo, C.L., 1997, "Numerical Study of a Backward-facing Step with Uniform Normal Mass Bleed," *Int. J. Heat and Mass Transfer*, Vol. 40, pp. 1677-1686.

Yang, J.T, and Tsai, C.H., 1996, "High Temperature Heat Transfer of Separated Flow over a Sudden Expansion with Base Mass Injection," *Int. J. Heat and Mass Transfer*, Vol.39, pp. 2293-2301.

Yang, J.T., Tsai, B.B., and Tsai, G.L., 1994, "Separated-Reattaching Flow Over a Backstep With Uniform Normal Mass Bleed," *Trans. ASME, Journal of Fluids Engineering*, Vol.116, pp.29-35